ACS Pharmacology & Translational Science

pubs.acs.org/ptsci

Article

Exploring the Protective Effect against 7,12-Dimethylbenz[a]anthracene-Induced Breast Tumors of Palmitoylethanolamide

Nilesh Rai, Vikas Kailashiya, and Vibhav Gautam*

Cite This: https://doi.org/10.1021/acsptsci.3c00188

Read Online

ACCESS | Metrics & More | Article Recommendations | Supporting Information

ABSTRACT: Breast cancer remains a global health burden, and the need for effective therapies is of chief importance. The current study explored the *in vivo* chemoprotective activity of palmitoylethanolamide (PEA) against 7,12-dimethylbenz-[a]anthracene (DMBA)-induced breast tumor in rats. Results of noninvasive photoacoustic imaging showed real-time progression in the tumor area and volume in DMBA-induced rats, while there was a reduction in tumor area and volume in PEA-treated tumor-bearing rats. The increase in the average oxygen saturation (sO_2 %) and decrease in the average total hemoglobin (HbT %) indicated the PEA-mediated attenuation of hypoxia-induced neovascularization in DMBA-induced rats. Histo-pathological investigations confirmed the efficacy of PEA in mitigating breast carcinoma, hepatotoxicity and nephrotoxicity driven by DMBA. Moreover, PEA-mediated alterations in the metabolic activity of the tumor microenvironment were evidenced by decreased glucose and lactate dehydrogenase enzyme level in the blood plasma and mammary tissue. PEA also maintained the redox balance by inhibiting nitric oxide level, reducing malondialdehyde (a product of lipid peroxidation), and increasing the level of antioxidant enzyme reduced glutathione. PEA altered the expression of apoptosis-related genes (*BAX*, *P53*,*BCL-XL*, *CASPASE-8*, and *CASPASE-9*) and induced the activity of Caspase-3 protein in the mammary tissue of tumor-bearing rats, indicating its apoptosis inducing ability. Taken together, the findings of this study suggest that PEA may have a protective effect against DMBA-induced breast tumors.

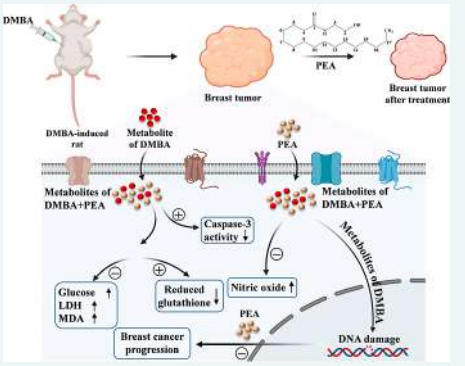

KEYWORDS: *breast cancer, palmitoylethanolamide, chemoprotective, redox balance, apoptosis*

Palmitoylethanolamide (PEA), a bioactive fatty acid compound belonging to the class of *N*-acyl-ethanolamines (NAEs), is extensively known to be used in neuropathic pain, allergy, and inflammation-mediated diseases. Additionally, PEA also exerts cytostatic properties in various models of cancer; not only that, but the signaling lipids related to PEA also play a substantial role in the regulation of cancer progression.[1] The ultramicronized PEA (um-PEA) induces apoptosis and regulates the growth of colon tumors by inducing fragmentation of DNA and arresting the cell cycle at G2/Mphase.[2] Moreover, PEA attenuates the expression level of fatty acid amide hydrolase and increases the apoptosis and antiproliferative effects of anandamide in cancer cells. Furthermore, PEA has been shown to reduce melanoma cell survival, induce apoptosis in high-grade neuroblastoma cells, and attenuate human brain tumor tissues. Although PEA is reported to be found endogenously, a study reports a decreased cellular level of PEA during cancer inflammation. In contrast to de novo lipogenesis, the breakdown of PEA-mediated by tumor cells led to the requirement of exogenous fatty acids, including palmitic acid. Therefore, the exogenously administered PEA could be an efficient approach toward the amelioration of cancer progression.

Breast cancer is a multifactorial, heterogeneous disease that alters the biochemistry, physiology, and molecular makeup of mammary tissues. Currently, breast cancer ranks as the fifth most common cause of cancer-related death and is one of the most often diagnosed malignancies in women worldwide. An estimated 2.3 million cases of breast cancer have been diagnosed worldwide, according to the statistics of GLOBOCAN 2020.[3] In transitioning countries, including Melanesia, Western Africa, Micronesia/Polynesia, and the Caribbean, breast cancer-related deaths are significantly higher, with an incidence rate approximately 88% than in transitioning countries such as Australia/New Zealand, Western Europe, Northern America, and Northern Europe. To detect and predict breast cancer at an early stage, imaging techniques such as photoacoustic (PA) imaging, ultrasonography, magnetic

Received: August 14, 2023
Revised: October 26, 2023
Accepted: October 31, 2023

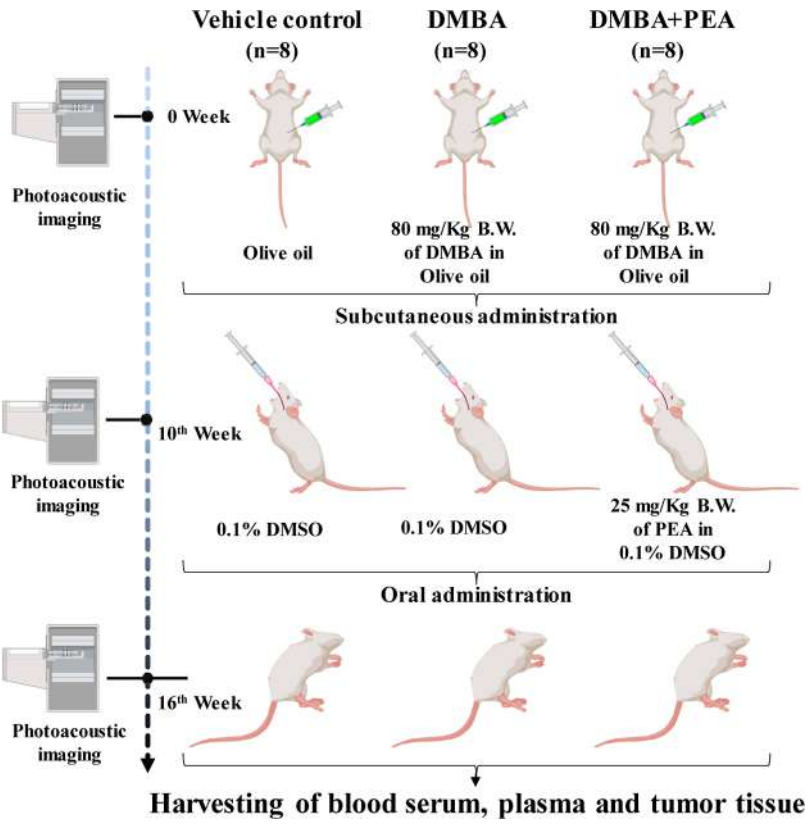

Figure 1. Schematic representation depicting a comprehensive overview of the experimental design and methodology.

resonance imaging (MRI), and mammography are commonly used.[4] Among these techniques, PA imaging has shown significant potential in clinical applications, particularly in oncology, as it enables early cancer detection, tumor characterization, and monitoring of treatment response.[4,5] Previous studies posited that the uncontrolled progression of breast cancer cells can be attributed to perturbations in multiple factors, including aberrant generation of reactive oxygen species (ROS), DNA damage, and exposure to ultraviolet (UV) radiation. These factors act by altering multiple pathways-related molecules, including the mitochondrial pathway, PI3K/AKT pathway, FasL/Fas pathway, nuclear factor-κB (NF-κB) pathway, and ROS-mediated pathway.[6] These cumulative effects promote the disruption of the delicate redox, proapoptotic, and antiapoptotic equilibrium, leading to dysregulated cell growth and evasion of apoptosis.[6,7] To potentially reduce the incidence rate of breast cancer and facilitate early treatment, the adoption of a chemotherapy-based preventive approach and the establishment of effective screening programs are deemed vital. The chemotherapeutic agents regulating the metabolic and molecular pathways involved in tumor cell growth and survival are being focused for breast cancer therapeutics. In the context of breast cancer progression, a complex signaling network encompassing multiple pivotal genes orchestrates the diverse facets of cellular integrity. Among these *BAX*, *BCL-XL*, *P53*, *CASPASE-8*, and *CASPASE-9* demonstrate distinct roles in the regulation of apoptosis. *BAX*, a pro-apoptotic member of the BCL-2 family, triggers apoptosis by creating pores in the mitochondrial membrane, allowing the release of Cyt-c, whereas *BCL-XL* opposes the release of Cyt-c. *CASPASE-8* and *CASPASE-9* are initiator caspases that play key roles in extrinsic and intrinsic apoptotic pathways, respectively. Whereas, *P53* activation may lead to the upregulation of pro-apoptotic genes like *BAX*, promoting apoptosis, and downregulation of antiapoptotic factors like *BCL-XL*. However, breast cancer is a highly diverse disease, and the precise interactions among these genes can vary depending on the subtype and genetic mutations present.

Till date, various therapeutic approaches, including chemotherapy, radiotherapy, chemo-radiotherapy, and surgery, have been employed for breast cancer treatment, but none of them offer a complete cure. Synthetic drugs used in chemotherapy have limitations, such as side effects, high toxicity, and damage to healthy cells near the tumor site. To overcome these limitations, natural lipid compounds have been explored as alternatives with better therapeutic efficacy and lower toxicity. However, despite efforts to use bioactive compounds derived from natural resources, a limited breakthrough has been achieved in breast cancer therapeutics.[7] Among these compounds, lipid mediators have shown pharmacological significance and have been used to combat various diseases including breast cancer. Previous studies report that chemotherapy induces peripheral neuropathic pain and other potential adverse effects, such as lymphedema, loss of weight, and discomfort. Additionally, the drug of cannabinoid nature with anti-inflammatory and analgesic properties may exert potential benefits in breast cancer-mediated inflammation and pain. PEA, an endocannabinoid-like lipid mediator, is recognized for its anti-inflammatory and neuroprotective properties.[8] A recent study reported that PEA docked to the active site of apoptosis-inducing proteins Bax, Bcl-2, P21, and P53, and *in vitro* findings suggest the cytotoxic and apoptosis-inducing ability of PEA against human breast cancer cells.[9] PEA exhibited enhanced pro-apoptotic activity in human

https://doi.org/10.1021/acsptsci.3c00188
ACS Pharmacol. Transl. Sci. XXXX, XXX, XXX−XXX

breast cancer cells, MDA-MB-231 and MCF-7, through the modulation of gene expression associated with the intrinsic (*BAX*, *BCL-2*, *P21*, and *P53*) and extrinsic (*CASPASE-8* and *FADD*) apoptotic pathways.[9] To the best of our knowledge, the preclinical therapeutic potential of PEA in the amelioration of DMBA-induced breast cancer progression is limited. Therefore, the present study endeavors to elucidate the ability of PEA to ameliorate the progression of breast cancer induced by DMBA through the regulation of metabolic processes and redox homeostasis, as well as modulating genes associated with apoptosis and tumor suppression.

MATERIALS AND METHODS

Animals and Drug Administration. Female Charles foster rats were obtained from the Central Animal Research Facility, Institute of Medical Sciences, Banaras Hindu University, Varanasi, India. The obtained rats were housed at the Centre of Experimental Medicine and Surgery, Institute of Medical Sciences, Banaras Hindu University, Varanasi, India. These rats were kept in a polypropylene cage, supplemented with a food pellet diet and water ad libitum, at a maintained temperature of 24 ± 2 °C with a 12 h light/dark cycle. The study was conducted in strict accordance with the guidelines prescribed by the Committee for Control and Supervision of Experiments on Animals (CCSEA), New Delhi, India. The Central Institutional Animal Ethics Committee of Banaras Hindu University, India, granted approval for the experimental protocols (Dean/2021/IAEC/3029 and Dean/2023/IAEC/6196).

Development of the *In Vivo* Breast Cancer Model. The *in vivo* study for the assessment of the anticancer properties of PEA was done using female Charles foster rats. The breast cancer was induced in female rats using subcutaneous administration of a single dose of 80 mg/kg body weight of 7,12-dimethylbenz[a]anthracene (DMBA).[10] The animals were divided into three groups, with 8 female rats in each group.

Group I served as vehicle control, subcutaneously treated with 300 μL of olive oil, and after 10 weeks 0.1% DMSO was administered orally thrice in a week.

Group II (DMBA) served as disease control, and the rats were given a single subcutaneous dose of DMBA (80 mg/kg body weight) in 300 μL of olive oil, and after 10 weeks 0.1% DMSO was given orally thrice in a week.

Group III (DMBA+PEA) was treated with DMBA, same as group II. After 10 weeks, 25 mg/kg body weight of PEA in 0.1% DMSO was given orally thrice in a week for the duration of next six weeks.

At the end of the experiment, the animals were sacrificed, and tumor tissues and blood from each group were collected for subsequent experiments (Figure 1). The administered single dose of DMBA effectively induces mammary tumors in rats with a 100% incidence rate, which was further confirmed by daily palpitations for the development of breast tumors. Moreover, the real-time progression of mammary cancer was monitored through PA imaging.

Photoacoustic Imaging. PA imaging was utilized to detect the presence of breast cancer at various time points.[11] The real-time monitoring of tumor size and tumor volume after PEA treatment was achieved through PA imaging. The B-mode and Oxy-Hemo PA-mode images were captured using a tunable laser operating platform within the range of 680 to 970 nm for the anatomical details and oxygen saturation parameter, respectively. Hemoglobin concentration and oxygen saturation level were quantified at a frequency of 21 MHz, in conjunction with a PA machine. Parameters such as tumor site localization and oxygen saturation (sO_2 %) were explored as potential cancer indicators, alongside quantification of total oxygen saturation and hemoglobin level.

Histopathological Analysis. The tumor tissues harvested from the respective groups were placed in 10% formalin solution. Thereafter, the paraffin blocks of each tissue were prepared, and thin sections of 10 μm were cut using microtome and placed onto glass slides. The tissue sections were deparaffinized using xylene, subjected to a gradient of ethanol solution for rehydration, and stained with hematoxylin and eosin (H&E) stain. Post-staining, the sections were cleared using alcohol/xylene (1:1), followed by xylene, and mounted with DPX permanently. Using a brightfield microscope (Olympus, CX43), images of sections were captured after H&E staining.[12]

Histopathological and Biochemical Analysis for Liver and Kidney Toxicity. Liver and kidney tissues were harvested from each groups and processed to prepare slides for H&E staining. The histopathological examination was done to assess the protective effects of PEA against DMBA-induced toxicity on the liver and kidneys. Thin sections (10 μm) of each tissue were sliced using a microtome, and H&E stained sections were subjected to image acquisition using a brightfield microscope (Olympus, CX43) for histopathological analysis. Further, liver function test and kidney function test were evaluated by examining the concentrations of aspartate aminotransferase (AST) and alanine aminotransferase (ALT), and urea and creatinine level in blood serum, as previously described.[13,14] The blood from rats of each group was collected after cardiac puncture and following centrifugation, and serum was collected and further tested for concentrations of AST, ALT, urea, and creatinine.

Estimation of Glucose and Lactate Dehydrogenase Level. Glucose is the foremost nutrient and energy source for cells to survive and proliferate. The equal quantity of protein extracted from blood plasma and mammary tissue of each group was used to estimate the glucose concentration using glucose estimation kit (Beacon Diagnostics, India) according to the instructions provided in kit. The absorbance was recorded at 505 nm and results for concentration of glucose was represented in μM in blood plasma and mammary tissue. The level of lactate dehydrogenase (LDH) in blood plasma and mammary tissue was estimated using Lactate Dehydrogenase Activity Assay Kit (E-BC-K046-S) by following manufacturer's instruction. The absorbance was recorded at 450 nm and results for concentration of LDH was represented in U/mL and U/mg of protein in blood plasma and mammary tissue, respectively.

Estimation of Nitric Oxide Production. The effect of PEA on DMBA-induced rats was evaluated to assess the alteration in nitric oxide production.[15] Nitric oxide is known to be involved as a signaling molecule in many cellular processes. Excess generation of NO is responsible to abrogate tumor growth and metastasis through the induction of apoptosis. The assessment of nitric oxide production was done using the Griess reagent that marks the accumulation of nitrite (NO_2^-), a stable NO metabolite. The equal quantity of protein extracted from blood plasma and mammary tissue was added with an equal volume of Griess reagent for 10 min; further absorbance was recorded at 540 nm, and the nitrite level was

https://doi.org/10.1021/acsptsci.3c00188
ACS Pharmacol. Transl. Sci. XXXX, XXX, XXX−XXX

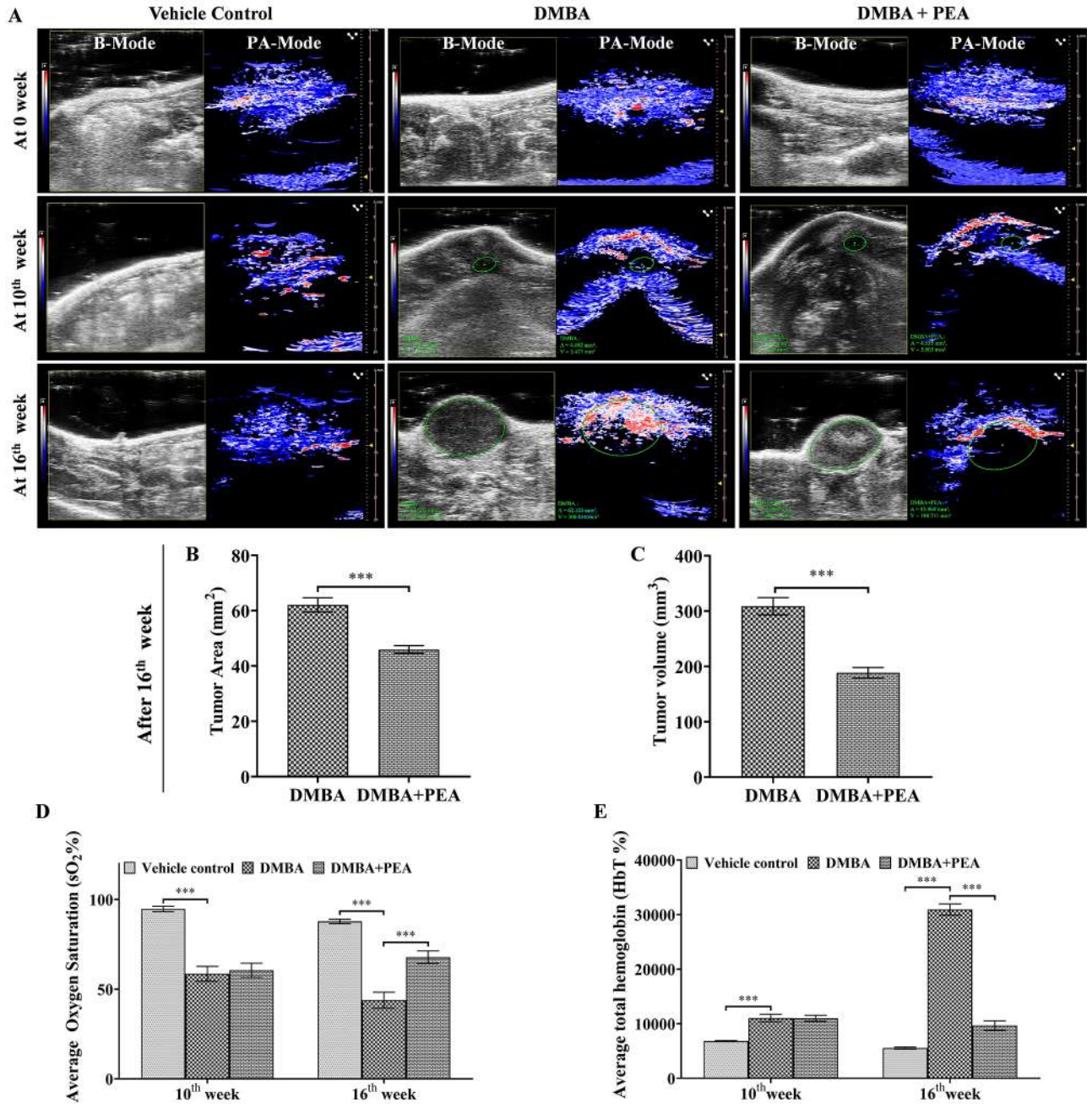

Figure 2. PA imaging shows real-time progression and PEA-mediated reduction in the DMBA-induced breast tumor. (A) PEA ameliorates the progression of breast tumors induced by DMBA in rats. PEA reduces the (B) tumor size and (C) volume and alters the level of (D) average oxygen saturation (sO_2 %) and (E) average total hemoglobin (HbT %) in DMBA-induced tumor-bearing rats. The data for tumor area and volume were presented as mean ± SEM ($n = 3$), and statistical significance (*$p < 0.050$, **$p < 0.010$, ***$p < 0.001$) was calculated using an unpaired Student's *t*-test. The data for average oxygen saturation and average total hemoglobin were presented as mean ± SEM ($n = 3$), and statistical significance (*$p \leq 0.033$, **$p \leq 0.002$, ***$p \leq 0.001$) was calculated using one-way ANOVA, followed by a post hoc Tukey test.

calculated using the standard curve of $NaNO_2$ (Figure S1). The results were expressed in μM/mL and μM/mg of protein in blood plasma and mammary tissue samples, respectively.

Estimation of Lipid Peroxidation. The impact of treatment on lipid peroxidation in DMBA-induced tumors was evaluated using a colorimetric method.[13] This method relies on the chemical reaction between malondialdehyde (MDA), an end product of lipid peroxidation, and thiobarbituric acid (TBA) to form a stable adduct under high temperature and acidic condition. Briefly, the blood plasma and mammary tissue from each group were harvested, and the mammary tissues were homogenized in 1× PBS to prepare tissue homogenate, which was centrifuged at 12,000*g* for 20 minutes at 4°C. Further, equal quantity of protein extracted from blood plasma and mammary tissue was incubated with 1 mL of a TBA solution (0.67%) and 3 mL of phosphoric acid (1%) at 70 °C for 120 min. Subsequently, the reaction mixture was cooled to room temperature, and the resulting product was extracted using 3 mL of methanol. After centrifugation at 3000 rpm at 4 °C for 10 min, the absorbance of the each extracted sample was recorded at 532 nm using a spectrophotometer. The concentration of MDA was calculated

https://doi.org/10.1021/acsptsci.3c00188
ACS Pharmacol. Transl. Sci. XXXX, XXX, XXX−XXX

after plotting a standard curve for MDA (Figure S2) and expressed in nM/mL and nM/mg of protein, respectively, in blood plasma and mammary tissue samples.

Estimation of Reduced Glutathione. The blood plasma and tissue homogenate from the respective groups were used for the estimation of reduced glutathione (GSH) following the previously described method with minor modifications.[16] Briefly, an equal quantity of protein extracted from blood plasma and mammary tissue was subjected to precipitation using 1 mL of GSH buffer (100 mM potassium phosphate buffer, pH 7.0, with 3 mM EDTA), followed by centrifugation at 1200*g* for 20 min. Subsequently, 0.5 mL of the resulting supernatant was mixed with 200 μL of GSH buffer, 100 μL of 5, 5′-dithiobis-(2-nitrobenzoic acid) (10 mM DTNB in methanol), and 200 μL methanol. The reaction mixture was left at room temperature, and the yellow-colored product that formed was measured immediately at 412 nm using a spectrophotometer. The concentration of GSH was calculated using standard curve of GSH (Figure S3) and expressed in μM/mL and μM/mg of protein, respectively, in blood plasma and mammary tissue samples.

Extraction of RNA and Quantitative Real Time-PCR (qRT-PCR) Analysis. The antibreast cancer activity induced by PEA in each group was confirmed by assessing the level of gene expression related to apoptosis (*BAX*, *CASPASE-8*, and *CASPASE-9*), cell survival (*BCL-XL*), and tumor suppression (*P53*) using qRT-PCR analysis. The standardized guidelines of MIQE were adhered to perform.[17] Total RNA was extracted from the mammary tissue of each group using the conventional TRIZOL method, and the concentration and purity of the extracted RNA were measured using a NanoDrop ONE (AZY1811395, Thermo Scientific, USA). A total of 5 μg of RNA from each vehicle control, DMBA-treated, and DMBA + PEA-treated group was used for cDNA synthesis utilizing the RevertAid First Strand cDNA Synthesis Kit (Thermo Fisher Scientific, USA) following the manufacturer's instructions. qRT-PCR amplification was performed using gene-specific primer (Table S1), PowerUp SYBR Green master mix (Thermo Fisher Scientific, USA), and synthesized cDNA on the QuantStudio 5 Real-Time PCR System. The β-actin gene served as the internal control for normalization. The qRT-PCR data were analyzed by comparing the ΔΔCT value, and the relative expression level for each gene was calculated using $2^{-\Delta\Delta CT}$ method.[18] The results are representative of three independent experiments.

Caspase-3 Activity Assay. The Caspase-3 activity was assessed in all three groups: the vehicle control group, the DMBA-treated group, and the DMBA + PEA-treated group. The estimation of the activity of Caspase-3 was conducted using the Caspase-3 activity assay kit (Elabscience, E-CK-A311A) according to the manufacturer's instructions. In brief, tissues from each group were harvested and homogenized in lysis buffer containing DTT. The homogenized tissues were centrifuged at 12,000*g* for 15 min at 4 °C, and the resulting supernatant containing protein was mixed with the reaction buffer and the substrate Ac-DEVDpNA, reaching a final volume of 100 μL. The reaction mixture was then incubated at 37 °C for 4 h. Following incubation, the absorbance was measured at 405 nm using a Multiskan microplate spectrophotometer (Thermo Fisher Scientific, USA), and the activity of Caspase-3 was expressed in fold change. The result represents data obtained from three independent experiments.[19]

Statistical Analysis. All the images and data were representative of three independent experiments. The data for tumor area and volume were presented as mean ± SEM, and an unpaired Student's *t*-test was performed to calculate the statistical significance ($^*p < 0.050$, $^{**}p < 0.010$, and $^{***}p < 0.001$) for DMBA + PEA-treated group when compared to the DMBA-treated group using GraphPad Prism 8.0 (San Diego, CA, USA). The results of quantitative measurements of metabolic parameters, oxidative parameters, antioxidant enzyme level, qRT-PCR data, and Caspase-3 activity were presented as mean ± SEM. The statistical significance among vehicle control, DMBA-treated, and DMBA + PEA-treated groups was performed using One-way ANOVA, and for qRT-PCR data Two-way ANOVA analyses followed by a post hoc Tukey test to determine the statistical significance ($^*p \leq 0.033$, $^{**}p \leq 0.002$, and $^{***}p \leq 0.001$) among vehicle control, DMBA-treated, and DMBA + PEA-treated groups.

RESULTS

PEA Attenuates the Tumor Area and Volume in DMBA-Induced Breast Tumor-Bearing Rats. PA imaging has shown significant potential in clinical applications, particularly in oncology, as it enables early cancer detection, tumor characterization, and monitoring of treatment response. One of the key advantages of PA imaging is its non-invasiveness, which minimizes patient discomfort and risk. In light of this, we performed PA imaging on all groups (Figure 2A), and our findings showed a significant reduction in tumor area and volume after the administration of PEA. The results of quantitative PI imaging after the 10th week indicated that there was no significant difference in tumor area, tumor volume, oxygen saturation (sO_2 %), and average total hemoglobin (HbT %) in DMBA treated and PEA-treated tumor bearing rats. On the other hand after the 16th week, the tumor area in the DMBA-induced rat was 62.10 ± 2.582 mm^2, whereas the tumor area was substantially reduced under the influence of PEA by 45.96 ± 1.392 mm^2 (*p*-value <0.001) (Figure 2B). On the contrary, the tumor area and volume in the vehicle control group were not observed, as no carcinogen was administered. Similarly, the tumor volume in the DMBA-induced rat was 308.81 ± 15.583 mm^3, and after the administration of PEA, it was substantially reduced to 188.71 ± 9.392 mm^3 (*p*-value <0.001) (Figure 2C).

Beside this, after 16th week we also evaluated the alteration in two additional parameters, average oxygen saturation (sO_2 %) and average total hemoglobin (HbT %), to validate the efficacy of PEA on DMBA-induced breast tumor progression. Interestingly, the decrease in the level of sO_2 % (43.85 ± 4.445%; *p*-value <0.001) was observed in DMBA-induced rats, as compared to the vehicle control group 87.79 ± 1.253%. On the other hand, the administration of PEA resulted in a rise in the sO_2 % level (67.84 ± 3.525%; *p*-value <0.001) in rats with breast tumors (Figure 2D). Likewise, after 16th week, the HbT % was observed to be 5541.70 ± 203.433% in the vehicle control group and found to be increased in DMBA-induced rats with 30933.22 ± 1033.228% (*p*-value <0.001). The level of HbT % was significantly decreased to 9662.55 ± 863.639% (*p*-value <0.001) after the administration of PEA in breast tumor-bearing rats (Figure 2E). The increased average oxygen saturation (sO_2 %) and decreased average total hemoglobin (HbT %) suggested PEA-mediated attenuation of hypoxia-induced neovascularization in DMBA-induced rats. Further, the histopathological investigations have substantiated the

https://doi.org/10.1021/acsptsci.3c00188
ACS Pharmacol. Transl. Sci. XXXX, XXX, XXX−XXX

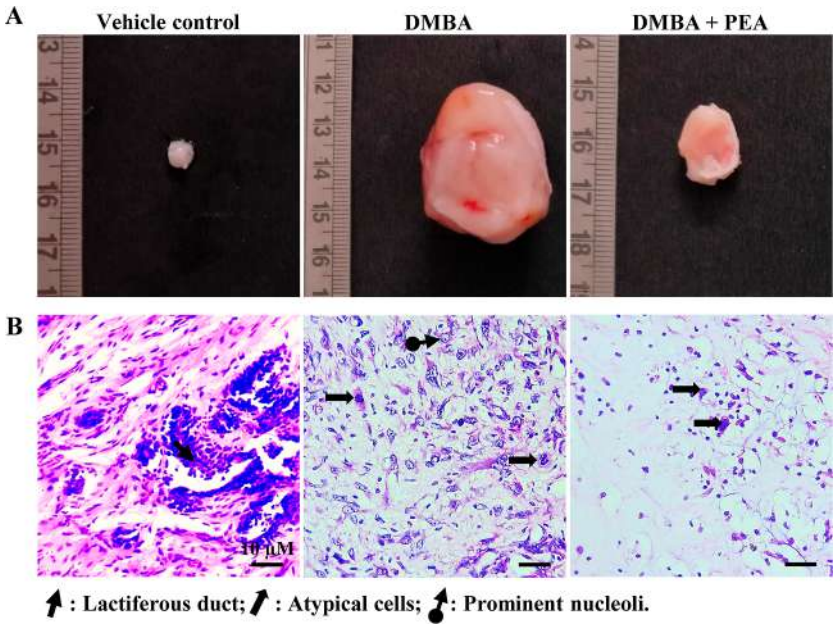

Figure 3. Illustrative image showing mammary tissue of vehicle control rats and the tumor size in DMBA-induced and PEA-treated breast tumor bearing rats. The image in lower panel showing the mammary tissue stained with hematoxylin and eosin for each respective group. (A) Tumor size reduces significantly in PEA-treated DMBA-induced breast tumor-bearing rats. (B) Histopathological examination shows that PEA improves the cellular morphology and reduces the number of atypical cells in DMBA-induced breast tumor-bearing rats. Scale bar = 10 μM.

efficacy of PEA in mitigating the breast carcinoma driven by DMBA in female Charles Foster rats.

PEA Alters the Morphology of Mammary Tissues in DMBA-Induced Breast Tumor-Bearing Rats. A histopathological examination was conducted to validate the results of a noninvasive study that suggested PEA-mediated suppression of DMBA-induced breast tumors. The tumor size was observed to be significantly reduced in DMBA-induced rats treated with PEA as compared to that in DMBA-treated rats (Figure 3A). The histological examination of DMBA-induced mammary tissue showed the breast tumor had markedly atypical cells with round to oval, markedly pleomorphic nuclei, prominent nucleoli, and many mitotic bodies. Additionally, it also showed the presence of spindle cell sarcomatous differentiation, suggesting a metaplastic breast carcinoma subtype, as compared to the vehicle control group, which showed the normal architecture of mammary tissue with overlying skin and lactiferous ducts. Conversely, when administered to rats with DMBA-induced tumors, PEA displayed therapeutic changes within tumor tissues, including the observation of necrotic foci, fibrosis, myxoid degeneration, and an infiltration of inflammatory cells. Furthermore, the presence of only a limited number of dispersed atypical cells was observed (Figure 3B).

PEA Reduces DMBA-Induced Hepatotoxicity and Renal Toxicity in Breast-Tumor Bearing Rats. DMBA-induced hepatotoxicity and renal toxicity result in significant histological alterations in the liver (Figure 4A) and kidney tissues (Figure 4D). These changes include the appearance of congestive blood vessels, necrosis, damage to the central vein, fibrosis in the liver, glomerular hypertrophy, and shrinkage of Bowman's space in the kidneys. On the other hand, the administration of PEA results in a reduction of such toxicity and enhances the condition of liver and kidney tissues. The marker enzymes present in the liver and kidney serve as a potential indicator of malignant cancer. Consequently, the blood serum of rats from each experimental group was assessed to determine the concentrations of liver marker enzymes (AST and ALT) and kidney marker enzymes (urea and creatinine).

When compared to vehicle control (155.12 ± 1.420 U/L), the level of serum AST was significantly increased to 290.77 ± 1.800 U/L (p-value <0.001) in DMBA-induced rats. However, the administration of PEA to DMBA-treated rats substantially declined the level of serum AST to 189.77 ± 2.980 U/L (p-value <0.001) (Figure 4B). Similarly, in comparison to the vehicle control group, where the level of ALT was noted as 28.00 ± 1.274 U/L, there was a significant elevation in serum ALT level to 56.00 ± 1.421 U/L (p-value <0.001) in rats induced with the potential carcinogen DMBA. Conversely, the administration of PEA to the DMBA-induced rats resulted in a substantial reduction in the level of serum ALT to 46.00 ± 1.262 U/L (p-value 0.001), signifying PEA-mediated potential mitigating effect against hepatotoxicity in rats induced by DMBA (Figure 4C). Moreover, in order to assess the renoprotective effect of PEA and corroborate the histopathological analysis of the kidney, the renal functional markers urea and creatinine were assessed. The analysis of renal function markers revealed a significant increase in the level of serum urea in DMBA-induced rats (47.31 ± 1.421 mg/dL; p-value <0.001), compared to the vehicle control group (33.20 ± 1.274 mg/dL). However, the administration of PEA led to a notable reduction in serum urea level (36.80 ± 1.262 mg/dL; p-value 0.003) as compared to DMBA-treated rats (Figure 4E). Similarly, the DMBA-induced rats displayed a significantly elevated level of serum creatinine, measuring at 0.51 ± 0.001 mg/dL (p-value <0.001), compared to the vehicle control group (0.28 ± 0.026 mg/dL). In contrast, the administration of PEA to the DMBA-induced rats substantially decreased the serum creatinine level to 0.38 ± 0.003 mg/dL (p-value 0.002) (Figure 4F). Overall, the administration of PEA effectively attenuated the elevated level of urea and creatinine induced by DMBA, suggesting its potential as a hepatoprotective and nephroprotective agent.

https://doi.org/10.1021/acsptsci.3c00188
ACS Pharmacol. Transl. Sci. XXXX, XXX, XXX−XXX

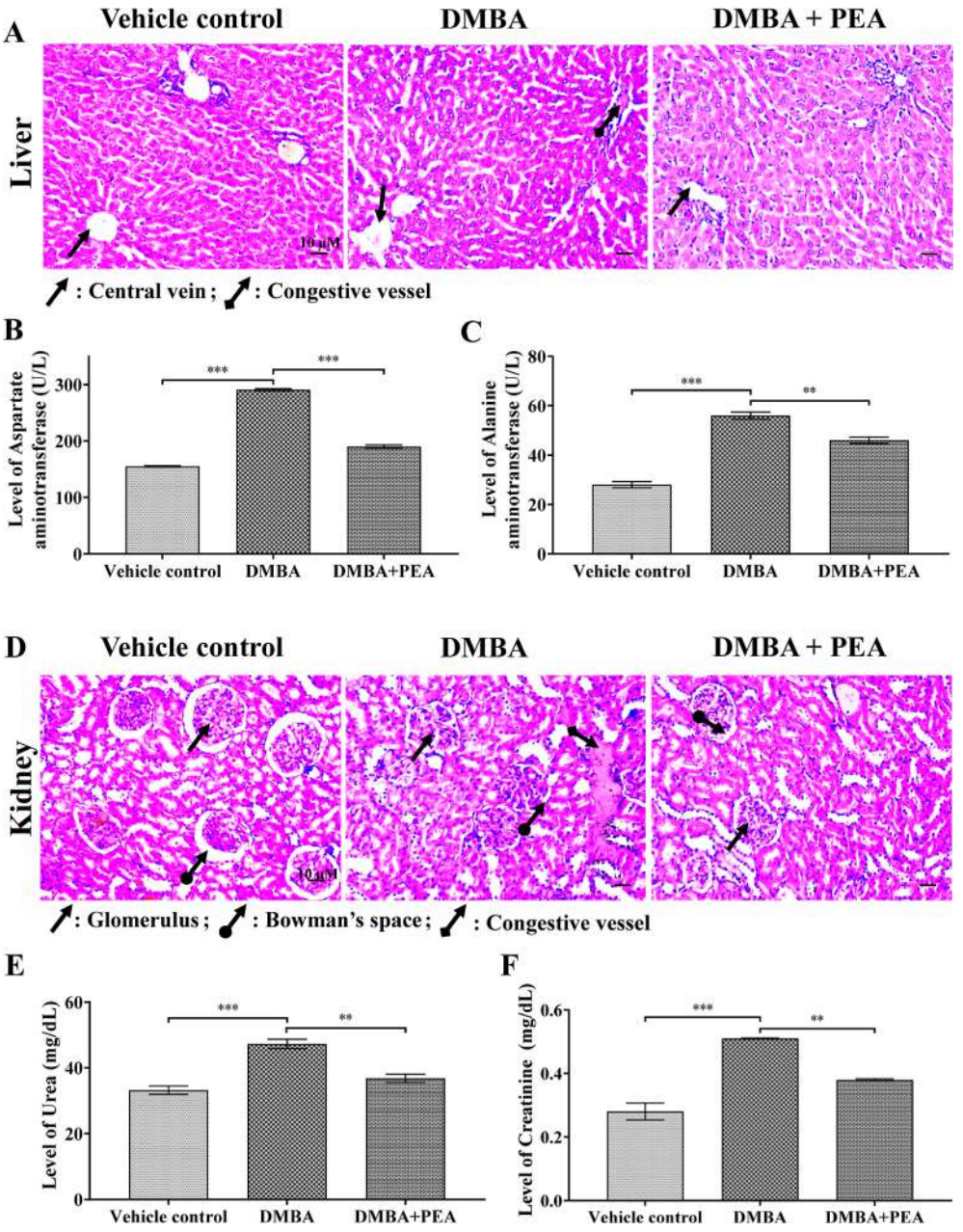

Figure 4. PEA improves the hepatic and renal architecture and maintains the level of liver and kidney markers in DMBA-induced breast tumor-bearing rats. (A) Histopathological examination of hepatic tissue showed improvement after PEA administration. The level of liver marker enzymes (B) AST and (C) ALT improved in the PEA-treated group as compared to DMBA-induced rats. (D) The histopathological analysis of renal tissue revealed improvement subsequent to the administration of PEA. PEA-treated tumor bearing rats showed improvement in level of renal markers (E) urea and (F) creatinine as compared to rats induced with DMBA only. The data for the quantification of AST, ALT, urea, and creatinine were represented as mean ± SEM (n = 3). Statistical significance was calculated using a one-way ANOVA followed by the Tukey post hoc test (*$p \leq$ 0.033, **$p \leq$ 0.002, ***$p \leq$ 0.001). Scale bar = 10 μM.

PEA Alters the Metabolic Activity in DMBA-Induced Breast Tumor-Bearing Rats. It is a well-proven fact that cancer cells primarily rely on aerobic glycolysis for energy production, even in the presence of oxygen. In other words, cancer cells obtain a significant portion of their energy through the conversion of glucose to lactate, followed by lactate fermentation. In light of these facts, we examined the concentrations of glucose and lactate dehydrogenase in blood plasma and mammary tissue of rats from each group to evaluate the effectiveness of PEA in combating breast cancer. The results revealed that the glucose level in the blood plasma and mammary tissues of DMBA-induced rats was significantly increased to 4829.34 ± 138.335 μM (p-value <0.001) and 7886.04 ± 94.200 μM (p-value <0.001), respectively as compared to the vehicle control group (880.52 ± 61.648 μM and 2119.13 ± 80.112 μM, respectively) (Figure 5A). However, the administration of PEA to DMBA-induced rats with breast tumors led to a decrease in glucose level in the blood plasma and mammary tissue microenvironment (2919.62 ± 52.640 μM; p-value <0.001 and 3454.83 ± 127.874 μM; p-value <0.001, respectively) (Figure 5B). Furthermore, we assessed the level of lactate dehydrogenase after PEA administration and observed a substantial increase in LDH level in the blood plasma of DMBA-induced rats (37.23

https://doi.org/10.1021/acsptsci.3c00188
ACS Pharmacol. Transl. Sci. XXXX, XXX, XXX−XXX

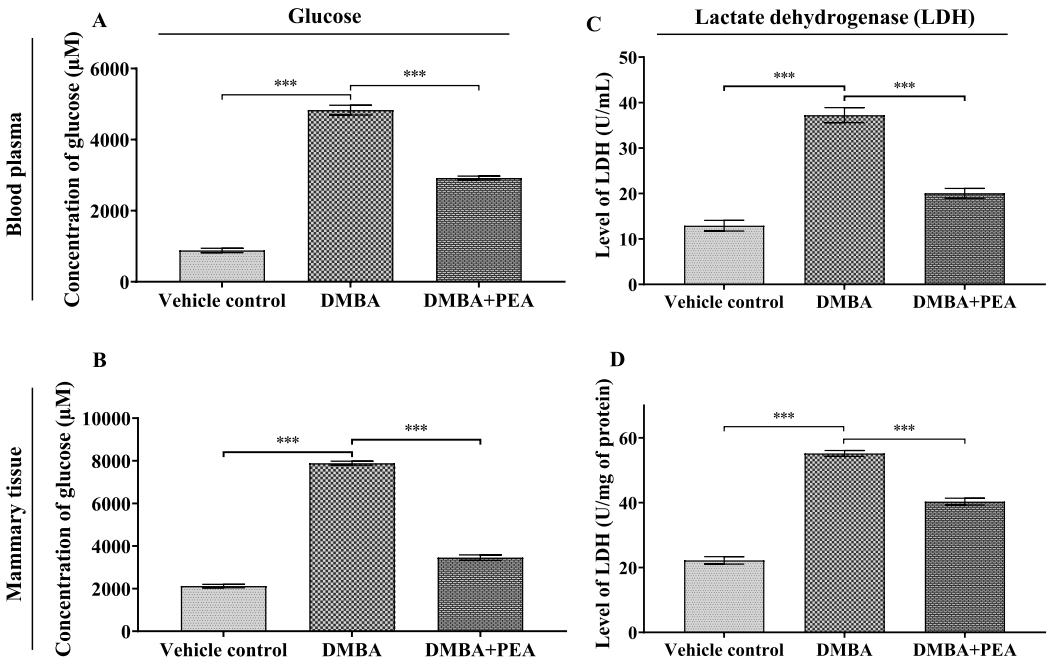

Figure 5. PEA exerts regulatory control over metabolic dysregulation observed in the blood plasma and mammary tissues of rats induced with DMBA. PEA decreases the concentration of glucose in (A) blood plasma and (B) mammary tissues of DMBA-induced breast tumor-bearing rats. Moreover, PEA exhibits the ability to reduce the level of lactate dehydrogenase enzyme in both the (C) blood plasma and (D) mammary tissues of breast tumor-bearing rats. The data were represented as the mean ± SEM (n = 3). Statistical significance was calculated using one-way ANOVA, followed by the Tukey post hoc test (*$p \leq 0.033$, **$p \leq 0.002$, ***$p \leq 0.001$).

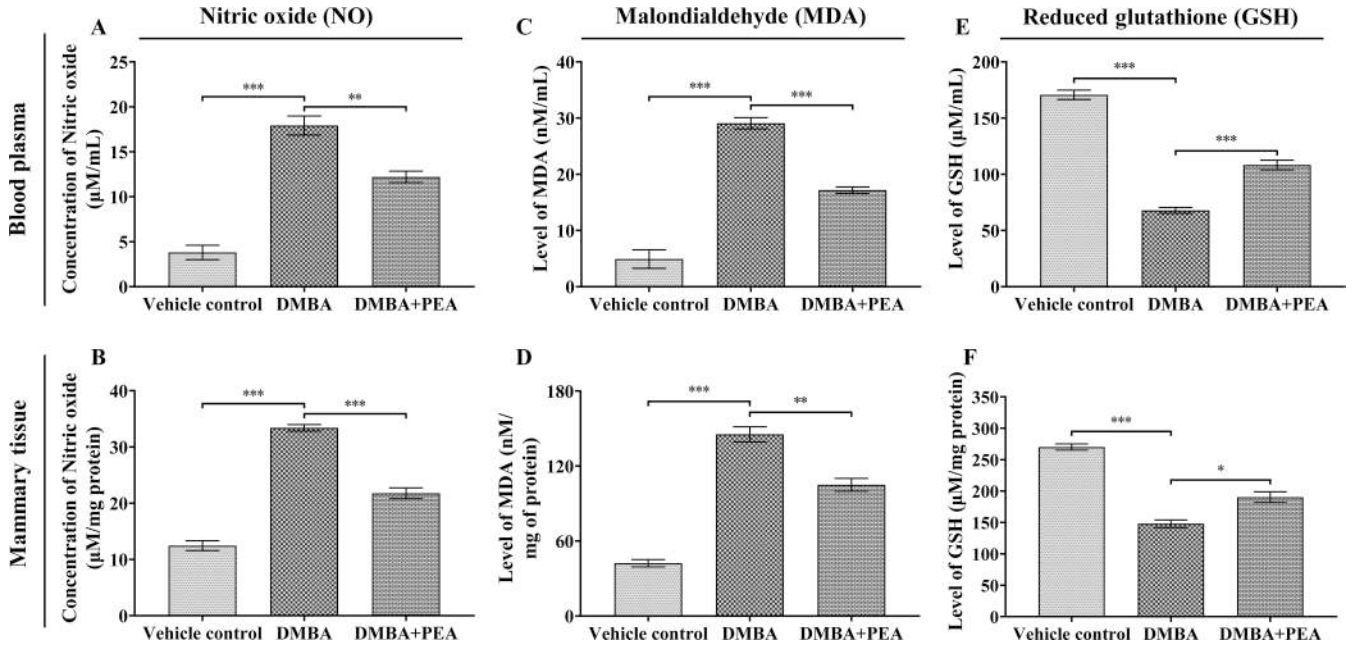

Figure 6. PEA exerts homeostatic control over the redox equilibrium in rats exposed to DMBA by modulating the concentration of oxidative stress-inducing agents and antioxidant enzymes in blood plasma and mammary tissue. PEA exerts a downregulatory effect on nitric oxide level in the (A) blood plasma and (B) mammary tissues of DMBA-induced breast tumor-bearing rats. Additionally, PEA demonstrates a capacity to attenuate the level of MDA in both the (C) blood plasma and (D) mammary tissues of rats with breast tumors. Conversely, PEA enhances the concentration of GSH in the (A) blood plasma and (B) mammary tissues of DMBA-induced rats. The data were represented as the mean ± SEM (n = 3). Statistical significance was calculated using a one-way ANOVA followed by a Tukey post hoc test (*$p \leq 0.033$, **$p \leq 0.002$, ***$p \leq 0.001$).

± 1.653 U/mL; p-value <0.001), compared to the vehicle control group (12.91 ± 1.164 U/mL). However, the administration of PEA resulted in a decrease in LDH level by 20.02 ± 1.083 U/mL (p-value <0.001) (Figure 5C). Similarly, the level of LDH in the mammary tissues of DMBA-induced rats was significantly higher (55.18 ± 0.901 U/mg of protein; p-value <0.001), compared to the vehicle control group (22.19 ± 1.150 U/mg of protein). Whereas, the administration of PEA to DMBA-induced rats led to a decrease

https://doi.org/10.1021/acsptsci.3c00188
ACS Pharmacol. Transl. Sci. XXXX, XXX, XXX−XXX

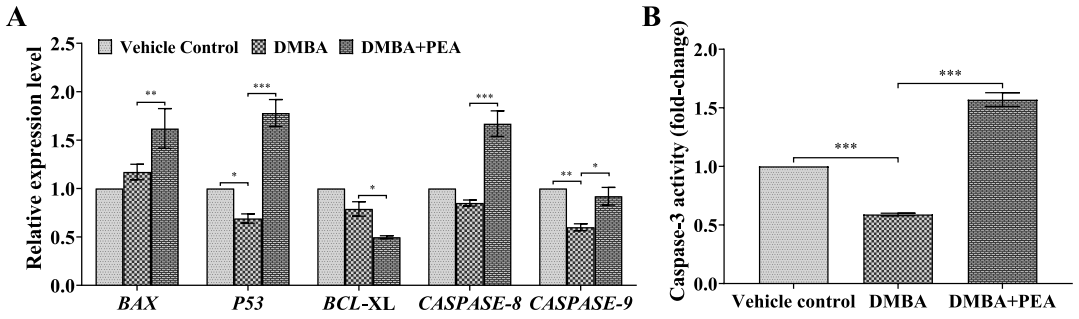

Figure 7. PEA elicits distinct modulation of apoptosis-related gene expression and induces an upregulation in the activity of Caspase-3. (A) PEA alters the expression of *BAX*, *P53*, *BCL-XL*, *CASPASE-8*, and *CASPASE-9*. (B) PEA enhances Caspase-3 activity in DMBA-induced tumor-bearing rats as compared to DMBA-induced rats. The data for relative expression level and Caspase-3 activity were represented as mean ± SEM (n = 3). Statistical significance was calculated using two-way ANOVA for qRT-PCR data one-way ANOVA for Caspase-3 activity followed by a Tukey post hoc test (*$p \leq 0.033$, **$p \leq 0.002$, and ***$p \leq 0.001$).

in LDH level in the mammary tissue microenvironment by 40.32 ± 1.063 U/mg of protein (p-value <0.001) (Figure 5D).

PEA Reduces the Level of Nitric Oxide and Malondialdehyde in DMBA-Induced Breast Tumor-Bearing Rats. Further, the study aimed to elucidate the status of oxidative stress parameters in DMBA-induced rats after the administration of PEA. The results demonstrated that DMBA abruptly induces the production of NO, 17.92 ± 1.061 μM/mL (p-value <0.001), in the blood plasma of the DMBA-treated group as compared to the vehicle control group, 3.80 ± 0.796 μM/mL. Whereas, in the blood plasma of PEA-treated tumor-bearing rats, the level of NO was decreased to 12.20 ± 0.642 μM/mL (p-value 0.008) (Figure 6A). Correspondingly, in DMBA-induced breast tumor tissue, the concentration of NO exhibited a significant elevation to 33.40 ± 0.578 μM/mg of protein (p-value <0.001), in contrast to the level of NO in the vehicle control group (12.45 ± 0.882 μM/mg of protein). Conversely, in the mammary tissue of tumor-bearing rats treated with PEA, the concentration of NO demonstrated a notable reduction to 21.76 ± 0.975 μM/mg of protein (p-value <0.001) (Figure 6B). Furthermore, the effect of PEA on DMBA-mediated lipid peroxidation was evaluated by determining the level of malondialdehyde (MDA), the end product of lipid peroxidation. Our findings revealed that the administration of DMBA resulted in an increase in the level of MDA in the blood plasma of the DMBA-treated rats at 29.08 ± 0.993 nM/mL (p-value <0.001), compared to the vehicle control group, which showed the concentration of MDA at 4.91 ± 1.664 nM/mL. Conversely, PEA decreased the level of MDA to 17.18 ± 0.567 nM/mL (p-value <0.001) in the blood plasma as compared to DMBA-induced tumor-bearing rats (Figure 6C). Additionally, the examination of MDA level in the mammary tissues of each group unveiled that DMBA significantly elevated the concentration of MDA (145.35 ± 6.067 nM/mg of protein; p-value <0.001) among DMBA-treated rats, whereas in rats of the vehicle control group, the MDA concentration was 42.18 ± 2.903 nM/mg of protein. On the other hand, PEA administration led to a reduction in MDA level (104.99 ± 5.062 nM/mg of protein; p-value 0.003) in the mammary tissues of rats with DMBA-induced tumors (Figure 6D).

PEA Increases the Level of Reduced Glutathione in DMBA-Induced Breast Tumor-Bearing Rats. The non-enzymatic antioxidant reduced glutathione (GSH) is known for its ability to counteract the overproduction of ROS, lipid peroxides, and other free radicals. Consequently, we assessed the level of GSH in the blood plasma and mammary tissue of rats from each experimental group. Our results demonstrated that the administration of DMBA led to a significant decrease in the concentration of GSH to 67.92 ± 2.610 μM/mL (p-value <0.001) in the blood plasma of DMBA-treated rats, as compared to the vehicle control group (170.71 ± 4.196 μM/mL). In contrast, the treatment with PEA elevated the GSH level to 108.25 ± 4.242 μM/mL (p-value <0.001) in the blood plasma of rats bearing tumors (Figure 6E). Furthermore, the examination of GSH level in the mammary tissues of each experimental group revealed that DMBA significantly decreased the concentration of GSH (147.92 ± 6.061 μM/mg of protein; p-value <0.001) in DMBA-treated rats. In contrast, the vehicle control group exhibited an increased GSH concentration with 270.00 ± 4.960 μM/mg of protein. Notably, the administration of PEA substantially increased the GSH level to 190.20 ± 8.642 μM/mg of protein (p-value 0.010) in the mammary tissues as compared to DMBA-induced rats (Figure 6F).

PEA Induces the Differential Gene Expression Associated with Apoptosis and Upregulates Caspase-3 Activity in DMBA-Induced Breast Tumor-Bearing Rats. Further, the study showed the expression of apoptosis-related genes in rats of each group to validate the apoptosis-inducing potential and DMBA-induced breast tumor-ameliorating potential of PEA (Figure 7A). The results demonstrated that, as compared to vehicle control (1-fold), the mRNA level of pro-apoptotic gene, *BAX*, in PEA-treated rats was significantly increased to 1.62 ± 0.205-fold (p-value 0.002) than that of DMBA-induced tumor-bearing rats (1.17 ± 0.08-fold; p-value 0.331), and the transcript expression of tumor-suppression gene *P53* in PEA-treated rats was upregulated by 1.78 ± 0.139-fold (p-value <0.001) as compared to DMBA-induced rats (0.69 ± 0.048-fold; p-value 0.034). Conversely, the expression of the antiapoptotic gene, *BCL-XL*, was downregulated by 0.497 ± 0.015-fold (p-value 0.048) in DMBA-induced rats administered with PEA. Whereas, the DMBA-induced rats exhibited an upregulation of *BCL-XL* expression by 0.79 ± 0.074 fold (p-value 0.189). Furthermore, the expression level of *CAPSASE-8* and *CAPSASE-9* genes in DMBA-induced rats administered with PEA was enhanced by 1.67 ± 0.132 (p-value <0.001) and 0.92 ± 0.091-fold (p-value 0.028), respectively, while the respective expressions were observed to be decreased by 0.85 ± 0.031 (p-value 0.420) and 0.60 ± 0.036-fold (p-value 0.005) in DMBA-induced rats. Considering the fact that PEA improves the breast cancer progression in DMBA-

https://doi.org/10.1021/acsptsci.3c00188
ACS Pharmacol. Transl. Sci. XXXX, XXX, XXX−XXX

induced rats by maintaining the redox balance and altering the expression of apoptosis related genes, the activity of executioner Caspase-3 was evaluated in the rats of each group. Wherein, the enzymatic activity of Caspase-3 in the mammary tissue of the vehicle control group was considered 1-fold. The activity of Caspase-3 was significantly increased in PEA-treated rats by 1.57 ± 0.059-fold (p-value <0.001) in comparison to DMBA-treated tumor-bearing rats (0.59 ± 0.011-fold; p-value <0.001) (Figure 7B).

DISCUSSION

Breast cancer, which is frequently detected and a significant contributor to cancer-related deaths among women globally, necessitates a comprehensive understanding of its underlying mechanisms for effective treatment and prevention.[20,21] Rodent models of breast cancer have emerged as valuable tools in this regard, offering crucial insights into the mechanisms driving disease development and potential therapeutic interventions.[22,23] The chemopreventive approach aims to inhibit or revert the progression of early-phase breast cancer to malignant carcinoma by employing synthetic or natural bioactive compounds.[24] The rationale underlying the present investigation was to evaluate the chemopreventive potential of PEA using a comparable experimental paradigm.[25,26] Among the different chemical-induced animal models available to study the diverse nature of breast cancer,[27] we selected the DMBA-induced female Charles Foster rat model of breast cancer. One of the frequently employed preclinical breast tumor models for the advancement of chemopreventive drugs in breast cancer therapeutics is DMBA-induced cancer model. Moreover, the mammary cancer induced by DMBA exhibits histogenesis, morphological characteristics, and biochemical features akin to the development of hyperplastic premalignant and malignant lesions observed in human breast cancer.[28,29] In addition, various events during cancer progression, such as tumor area and volume, can be attributed to several physiological, biochemical, and molecular alterations. In our study, the histopathological analysis provided additional evidence of the efficacy of PEA in mitigating breast carcinoma driven by DMBA in female Charles Foster rats, reinforcing the observed results of reduced tumor size, tumor area, and volume. Furthermore, the findings of elevated sO_2 % and attenuated HbT % level collectively demonstrate the potential therapeutic benefit of PEA by modulating tumor-associated hypoxia and neovascularization. The noninvasive nature of PA imaging technique makes it a valuable tool in assessing the effects of PEA and highlights its potential as a safer and more effective alternative in breast cancer detection and management.

Biomarkers are widely utilized to monitor cancerous conditions, particularly to assess responses to pharmacotherapy. Upon exposure to carcinogens, cells experience structural damage, resulting in the leakage of cytoplasmic enzymes into the bloodstream. AST, ALT, urea, creatinine, and LDH are pathophysiological diagnostic markers employed to measure the extent of liver and kidney damage. The increased functional activities of AST, ALT, urea, creatinine, and LDH may primarily stem from liver cytosol leakage into the blood due to tissue injury, which is a hallmark feature in a cancerous environment.[30,31] The present study showed the elevated level of liver enzymes such as AST and ALT in mammary cancer, implying tumor growth and hepatotoxicity induced by DMBA. Similarly, increased serum urea and creatinine concentrations were attributed to DMBA-induced kidney toxicity. LDH is recognized as a potential marker enzyme for evaluating the progression of proliferating malignant cells, as numerous studies have reported increased LDH level in various cancers.[32] The elevated LDH and glucose level can also be attributed to the high rate of glycolysis under anaerobic conditions in the cancerous state, which provides the only energy-generating pathway for the uncontrolled division of malignant cells.[31,33] In this study, DMBA-induced breast-tumor-bearing rats exhibited an upsurge in glucose and LDH concentrations, indicative of susceptible growth and high enzyme production by proliferated cells, making them sensitive markers for solid neoplasms. Furthermore, PEA treatment decreased the elevated level of AST, ALT, urea, and creatinine in serum as well as the increased concentration of LDH and glucose in blood plasma and tumor tissue in breast cancer-induced rats. The observed decrease in glucose and LDH level in both blood plasma and mammary tissue in DMBA-induced breast tumor-bearing rats can be attributed to a multifaceted interplay of metabolic, hormonal, and physiological alterations, which collectively contribute to an alteration in tumor metabolism and inflammatory responses. Therefore, PEA-mediated depletion of glucose and LDH in both blood plasma and mammary tissue indicates its breast cancer-preventing activity. Additionally, the administration of PEA led to noticeable improvements in the cellular architecture of liver, kidney, and mammary tissue, suggesting its potential as an antibreast cancer agent. Overall, the improved tissue architecture and the restoration of various biochemical markers indicate the potential of PEA to ameliorate the progression of breast tumor progression.

DMBA, a polycyclic aromatic hydrocarbon, undergoes metabolic activation in the body, primarily in the liver, through the action of cytochrome P450 enzymes.[34] These enzymes convert DMBA into highly reactive metabolites, including dihydrodiol epoxides. The metabolites of DMBA are accountable for the production of ROS, thereby initiating the generation of unpaired electrons known as free radicals, ultimately culminating in the exhaustion of antioxidant defenses. This process subsequently triggers lipid peroxidation within cellular membranes, consequently instigating alterations in the genetic material (DNA), prompting augmented cellular proliferation, and ultimately contributing to the intricate process of mammary carcinogenesis.[35] Nitric oxide (NO), a signaling molecule involved in diverse physiological processes, exerts its influence by interacting with various targets, including enzymes and signaling pathways.[36,37] In particular, NO has been shown to modulate the activity of glutathione peroxidases (GPx), an enzyme critically involved in cellular antioxidant defense mechanisms. For instance, the potential nitric oxide donor *S*-nitroso-*N*-acetyl penicillamine (SNAP) has demonstrated the ability to inhibit GPx activity in specific cell types, such as U937 cells.[38] This inhibition disrupts the delicate equilibrium between oxidants and antioxidants within the cell, thereby leading to an elevated level of lipid peroxidation.[39] GPx employs the reducing potential of the tripeptide glutathione (GSH) to detoxify peroxides. Furthermore, oxidative stress induced by ROS or other free radicals, including nitric oxide, triggers the formation of malondialdehyde (MDA) and other aldehydes through the process of lipid peroxidation. DMBA-mediated lipid peroxidation plays a pivotal role in the progression, promotion, and development of breast cancer progression.[40] In rats induced with DMBA, treatment with PEA significantly alleviated oxidative stress by

https://doi.org/10.1021/acsptsci.3c00188
ACS Pharmacol. Transl. Sci. XXXX, XXX, XXX−XXX

reducing MDA level compared with the DMBA-induced rats. Intriguingly, treatment with PEA in DMBA-induced rats resulted in enhanced GSH activity compared to that in DMBA-induced breast tumor rats.

Apoptosis represents a process of programmed cell death that can be activated in response to intracellular (intrinsic apoptosis) or extracellular (extrinsic apoptosis) signaling molecules.[41] The biochemical hallmarks of this intricate cellular phenomenon encompass loss of cellular and nuclear integrity, alteration in metabolic activity and oxidative molecules, DNA fragmentation, differential expression of apoptosis-inducing genes and proteins, and the formation of entities known as apoptotic bodies.[42−44] *BAX*, a noteworthy pro-apoptotic gene, instigates the initiation of programmed cell death by initiating the release of Cyt-c from mitochondria. The antiapoptotic *BCL-XL* gene, which plays a crucial role within the *BCL-2* family, hinders apoptosis by preventing the release of Cyt-c. In our study, we report PEA-mediated upregulation in the expression of the proapoptotic gene *BAX* and downregulation in the expression of the *BCL-XL* gene in DMBA-induced rats. Another pivotal gene, *P53*, plays a critical role in eliciting notable responses such as tumor suppression and the initiation of apoptosis through two major pathways known as the intrinsic mitochondrial pathway and the extrinsic death receptor pathway.[45] Perturbations in *P53* can compromise its tumor-suppressive efficacy.[46] Our study exhibited the upregulation of the *P53* gene in DMBA-induced breast cancer rats treated with PEA, suggesting its tumor suppression role. Caspase-8 serves as an initiator caspase, participates in the extrinsic apoptotic pathway, and activates downstream effector caspases, including Caspase-3. Conversely, *CASPASE-9* acts as an initiator caspase in the intrinsic apoptotic pathway, being activated by the release of Cyt-c. It assembles the apoptosome complex, subsequently eliciting the activation of effector caspases. Similarly, a previous finding showed that 18β-glycyrrhetinic acid initiates apoptosis in human breast cancer cells (MCF-7) via the activation of the mitochondrial apoptotic pathway, marked by the loss of mitochondrial membrane potential, which subsequently facilitated the release of Cyt-c and the subsequent activation of Caspase-9.[47] Furthermore, the increase in the expression of *CASPASE-8* and *CASPASE-9* genes in DMBA-induced breast cancer rats treated with PEA, as well as an increase in the activity of Caspase-3 protein, indicates antibreast cancer potentiation of PEA. Taken together, our study highlights the potential of PEA as a promising chemopreventive agent for breast cancer management.

CONCLUSIONS

The current study provides compelling evidence showcasing the potential antibreast tumor potential of PEA. The results obtained through PA imaging demonstrate a reduction in both the tumor area and volume. Simultaneously, there is an increase in sO_2 % level and a decrease in HbT % level. These findings strongly suggest that PEA effectively curbs hypoxia-induced neovascularization in rats afflicted with DMBA-induced breast tumors. Histopathological examinations further affirm the efficacy of PEA, showing its capacity to alleviate the progression of DMBA-triggered breast carcinoma. Moreover, PEA exerts an impact on metabolic activity, evident by the diminished level of glucose and lactate dehydrogenase enzyme in both blood plasma and mammary tissue of DMBA-induced rats. Additionally, PEA plays a role in maintaining the redox equilibrium in blood plasma and mammary tissue, which is evidenced by its inhibitory effect on nitric oxide level, reduction of malondialdehyde level, and elevation of the antioxidant enzyme reduced glutathione. Furthermore, PEA induces alterations in the expression of apoptosis-related genes, including *BAX*, *P53*, *BCL-XL*, *CASPASE-8*, and *CASPASE-9*. It also enhances the activity of the Caspase-3 protein, indicating its ability to induce apoptosis in DMBA-induced breast tumors. In summary, comprehensive *in vivo* studies offer compelling scientific support for considering PEA as a potential therapeutic agent in breast cancer treatment. Moving forward, additional research should delve into identifying specific molecules and signaling pathways associated with apoptosis and breast tumor progression that are modulated by PEA.

ASSOCIATED CONTENT

Data Availability Statement

Supporting data for the findings of this study can be found in the Supporting Information accompanying this article.

Supporting Information

The Supporting Information is available free of charge at https://pubs.acs.org/doi/10.1021/acsptsci.3c00188.

List of primers used in the qRT-PCR study; standard curve of sodium nitrite; standard curve of the malondialdehyde; standard curve of the GSH (PDF)

AUTHOR INFORMATION

Corresponding Author

Vibhav Gautam − *Centre of Experimental Medicine and Surgery, Institute of Medical Sciences, Banaras Hindu University, Varanasi 221005, India;* orcid.org/0000-0001-7956-9555; Phone: +918860182113; Email: vibhav.gautam4@bhu.ac.in, vibhavgautam16@gmail.com

Authors

Nilesh Rai − *Centre of Experimental Medicine and Surgery, Institute of Medical Sciences, Banaras Hindu University, Varanasi 221005, India;* orcid.org/0000-0003-0431-9150

Vikas Kailashiya − *Department of Pathology, Institute of Medical Sciences, Banaras Hindu University, Varanasi 221005, India*

Complete contact information is available at: https://pubs.acs.org/10.1021/acsptsci.3c00188

Author Contributions

Nilesh Rai—data curation, formal analysis, investigation, methodology, roles/writing-original draft, software, writing-review and editing, and visualization. Vikas Kailashiya—data curation. Vibhav Gautam—conceptualization, methodology, formal analysis, funding acquisition, investigation, project administration, resources, supervision, and writing—review and editing.

Funding

The funding for V.G.'s laboratory is derived from financial support provided by the Institution of Eminence Seed Grant and Bridge Grant at Banaras Hindu University (BHU), India, the University Grants Commission, New Delhi, India, and the Science and Engineering Research Board (SERB)-EMEQ grant (EEQ/2019/000025).

Notes

The authors declare no competing financial interest.

■ ACKNOWLEDGMENTS

N.R. expresses gratitude to the University Grants Commission, New Delhi, India, for the Junior and Senior Research Fellowship. V.G. expresses gratitude for the financial backing extended to his laboratory from the Institution of Eminence Seed Grant and Bridge Grant at Banaras Hindu University (BHU), India, the University Grants Commission, New Delhi, India, and the Science and Engineering Research Board (SERB)-EMEQ grant (EEQ/2019/000025). The corresponding author, representing all contributors, extends appreciation to the SATHI-BHU Centre for granting access to the photoacoustic imaging facility. Figure 1, showing the work plan and the table of content graphics, was created using www.biorender.com.

■ REFERENCES

(1) Pisanti, S.; Picardi, P.; D'Alessandro, A.; Laezza, C.; Bifulco, M. The endocannabinoid signaling system in cancer. *Trends Pharmacol. Sci.* **2013**, *34* (5), 273−282.

(2) Pagano, E.; Venneri, T.; Lucariello, G.; Cicia, D.; Brancaleone, V.; Nanì, M. F.; Cacciola, N. A.; Capasso, R.; Izzo, A. A.; Borrelli, F.; Romano, B. Palmitoylethanolamide Reduces Colon Cancer Cell Proliferation and Migration, Influences Tumor Cell Cycle and Exerts *In Vivo* Chemopreventive Effects. *Cancers (Basel)* **2021**, *13* (8), 1923.

(3) Sung, H.; Ferlay, J.; Siegel, R. L.; Laversanne, M.; Soerjomataram, I.; Jemal, A.; Bray, F. Global Cancer Statistics 2020: GLOBOCAN Estimates of Incidence and Mortality Worldwide for 36 Cancers in 185 Countries. *Ca-Cancer J. Clin.* **2021**, *71* (3), 209−249.

(4) Tsarouchi, M. I.; Hoxhaj, A.; Mann, R. M. New Approaches and Recommendations for Risk-Adapted Breast Cancer Screening. *J. Magn. Reson. Imaging* **2023**, *58* (4), 987−1010.

(5) Kitai, T.; Torii, M.; Sugie, T.; Kanao, S.; Mikami, Y.; Shiina, T.; Toi, M. Photoacoustic mammography: initial clinical results. *Breast Cancer* **2014**, *21*, 146−153.

(6) Rajabi, S.; Maresca, M.; Yumashev, A. V.; Choopani, R.; Hajimehdipoor, H. The most competent plant-derived natural products for targeting apoptosis in cancer therapy. *Biomolecules* **2021**, *11* (4), 534.

(7) Estrela, J. M.; Mena, S.; Obrador, E.; Benlloch, M.; Castellano, G.; Salvador, R.; Dellinger, R. W. Polyphenolic phytochemicals in cancer prevention and therapy: bioavailability versus bioefficacy. *J. Med. Chem.* **2017**, *60* (23), 9413−9436.

(8) Petrosino, S.; Di Marzo, V. The pharmacology of palmitoylethanolamide and first data on the therapeutic efficacy of some of its new formulations. *Br. J. Pharmacol.* **2017**, *174* (11), 1349−1365.

(9) Rai, N.; Gupta, P.; Verma, A.; Singh, S. K.; Gautam, V. Isolation and characterization of N-(2-Hydroxyethyl)hexadecanamide from *Colletotrichum gloeosporioides* with apoptosis-inducing potential in breast cancer cells. *BioFactors* **2023**, *49* (3), 663−683.

(10) Shaban, N. Z.; El-Rashidy, F. H.; Adam, A. H.; Beltagy, D. M.; Ali, A. E.; Abde-Alaziz, A. A.; Talaat, I. M. Anticancer role of mango (*Mangifera indica* L.) peel and seed kernel extracts against 7, 12-dimethylbenz [a] anthracene-induced mammary carcinogenesis in female rats. *Sci. Rep.* **2023**, *13* (1), 7703.

(11) Zhang, J.; Duan, F.; Liu, Y.; Nie, L. High-resolution photoacoustic tomography for early-stage cancer detection and its clinical translation. *Radiol.: Imaging Cancer* **2020**, *2* (3), No. e190030.

(12) Karnam, K. C.; Ellutla, M.; Bodduluru, L. N.; Kasala, E. R.; Uppulapu, S. K.; Kalyankumarraju, M.; Lahkar, M. Preventive effect of berberine against DMBA-induced breast cancer in female Sprague Dawley rats. *Biomed. Pharmacother.* **2017**, *92*, 207−214.

(13) Wang, Z.; Zhang, X. Chemopreventive Activity of Honokiol against 7, 12 - Dimethylbenz[a]anthracene-Induced Mammary Cancer in Female Sprague Dawley Rats. *Front. Pharmacol.* **2017**, *8*, 320.

(14) Bergmeyer, H.; Scheibe, P.; Wahlefeld, A. Optimization of methods for aspartate aminotransferase and alanine aminotransferase. *Clin. Chem.* **1978**, *24* (1), 58−73.

(15) Kumar, S.; Kashyap, P. Antiproliferative activity and nitric oxide production of a methanolic extract of *Fraxinus micrantha* on Michigan Cancer Foundation-7 mammalian breast carcinoma cell line. *J. Intercult. Ethnopharmacol.* **2015**, *4* (2), 109−113.

(16) Bethu, M. S.; Netala, V. R.; Domdi, L.; Tartte, V.; Janapala, V. R. Potential anticancer activity of biogenic silver nanoparticles using leaf extract of *Rhynchosia suaveolens*: an insight into the mechanism. *Artif. Cells, Nanomed., Biotechnol.* **2018**, *46* (sup1), 104−114.

(17) Bustin, S. A.; Benes, V.; Garson, J. A.; Hellemans, J.; Huggett, J.; Kubista, M.; Mueller, R.; Nolan, T.; Pfaffl, M. W.; Shipley, G. L.; Vandesompele, J.; Wittwer, C. T. The MIQE Guidelines: Minimum Information for Publication of Quantitative Real-Time PCR Experiments. *Clin. Chem.* **2009**, *55* (4), 611−622.

(18) Gautam, V.; Singh, A.; Yadav, S.; Singh, S.; Kumar, P.; Sarkar Das, S.; Sarkar, A. K. Conserved LBL1-ta-siRNA and miR165/166-RLD1/2 modules regulate root development in maize. *Development* **2020**, *148* (1), dev190033.

(19) Mishra, E.; Thakur, M. K. Mdivi-1 Rescues Memory Decline in Scopolamine-Induced Amnesic Male Mice by Ameliorating Mitochondrial Dynamics and Hippocampal Plasticity. *Molecular Neurobiology* **2023**, *60*, 5426−5449.

(20) Winters, S.; Martin, C.; Murphy, D.; Shokar, N. K. Breast cancer epidemiology, prevention, and screening. *Prog. Mol. Biol. Transl. Sci.* **2017**, *151*, 1−32.

(21) Azadnajafabad, S.; Saeedi Moghaddam, S.; Keykhaei, M.; Shobeiri, P.; Rezaei, N.; Ghasemi, E.; Mohammadi, E.; Ahmadi, N.; Ghamari, A.; Shahin, S.; et al. Expansion of the quality of care index on breast cancer and its risk factors using the Global Burden of Disease Study 2019. *Cancer Med.* **2023**, *12* (2), 1729−1743.

(22) Singhal, S. S.; Garg, R.; Mohanty, A.; Garg, P.; Ramisetty, S. K.; Mirzapoiazova, T.; Soldi, R.; Sharma, S.; Kulkarni, P.; Salgia, R. Recent Advancement in Breast Cancer Research: Insights from Model Organisms—Mouse Models to Zebrafish. *Cancers* **2023**, *15* (11), 2961.

(23) Russo, J.; Gusterson, B. A.; Rogers, A. E.; Russo, I. H.; Wellings, S. R.; Van Zwieten, M. J. Comparative Study of Human and Rat Mammary Tumorigenesis. In *Pathology Reviews • 1990*; Rubin, E., Damjanov, I., Eds.; Humana Press: Totowa, NJ, 1990; pp 217−251.

(24) Jordan, V. C.; Morrow, M. Tamoxifen, Raloxifene, and the Prevention of Breast Cancer*. *Endocr. Rev.* **1999**, *20* (3), 253−278.

(25) Sahin, K.; Tuzcu, M.; Sahin, N.; Akdemir, F.; Ozercan, I.; Bayraktar, S.; Kucuk, O. Inhibitory Effects of Combination of Lycopene and Genistein on 7,12- Dimethyl Benz(a)anthracene-Induced Breast Cancer in Rats. *Nutr. Cancer* **2011**, *63* (8), 1279−1286.

(26) Mandal, A.; Bishayee, A. *Trianthema portulacastrum* Linn. Displays Anti-Inflammatory Responses during Chemically Induced Rat Mammary Tumorigenesis through Simultaneous and Differential Regulation of NF-κB and Nrf2 Signaling Pathways. *Int. J. Mol. Sci.* **2015**, *16* (2), 2426−2445.

(27) Machida, Y.; Imai, T. Different properties of mammary carcinogenesis induced by two chemical carcinogens, DMBA and PhIP, in heterozygous BALB/*c Trp53* knockout mice. *Oncol. Lett.* **2021**, *22* (4), 738.

(28) Witty, J. P.; Lempka, T.; Coffey, R. J., Jr.; Matrisian, L. M. Decreased tumor formation in 7,12-dimethylbenzanthracene-treated stromelysin-1 transgenic mice is associated with alterations in mammary epithelial cell apoptosis. *Cancer Res.* **1995**, *55* (7), 1401−1406.

(29) Costa, I.; Solanas, M.; Escrich, E. Histopathologic characterization of mammary neoplastic lesions induced with 7,12 dimethylbenz(alpha)anthracene in the rat: a comparative analysis with human breast tumors. *Arch. Pathol. Lab. Med.* **2002**, *126* (8), 915−927.

https://doi.org/10.1021/acsptsci.3c00188
ACS Pharmacol. Transl. Sci. XXXX, XXX, XXX−XXX

(30) Yam, L. T.; Janckila, A. J.; Chan, C. H.; Li, C. Y. Hepatic involvement in hairy cell leukemia. *Cancer* **1983**, *51* (8), 1497−1504.
(31) Divakaruni, A. S.; Wiley, S. E.; Rogers, G. W.; Andreyev, A. Y.; Petrosyan, S.; Loviscach, M.; Wall, E. A.; Yadava, N.; Heuck, A. P.; Ferrick, D. A.; et al. Thiazolidinediones are acute, specific inhibitors of the mitochondrial pyruvate carrier. *Proc. Natl. Acad. Sci. U.S.A.* **2013**, *110* (14), 5422−5427.
(32) Forkasiewicz, A.; Dorociak, M.; Stach, K.; Szelachowski, P.; Tabola, R.; Augoff, K. The usefulness of lactate dehydrogenase measurements in current oncological practice. *Cell. Mol. Biol. Lett.* **2020**, *25* (1), 35.
(33) Lakshmi, A.; Subramanian, S. Chemotherapeutic effect of tangeretin, a polymethoxylated flavone studied in 7, 12-dimethylbenz-(a)anthracene induced mammary carcinoma in experimental rats. *Biochimie* **2014**, *99*, 96−109.
(34) Lin, Y.; Yao, Y.; Liu, S.; Wang, L.; Moorthy, B.; Xiong, D.; Cheng, T.; Ding, X.; Gu, J. Role of mammary epithelial and stromal P450 enzymes in the clearance and metabolic activation of 7,12-dimethylbenz(a)anthracene in mice. *Toxicol. Lett.* **2012**, *212* (2), 97−105.
(35) Mani, G.; Arumugam, M.; Maril, A.; Devaki, T. Naringin attenuates DMBA-induced mammary carcinogenesis in rats via regulating the oxidative stress and antioxidants status. *J. Chem. Pharm. Res.* **2018**, *10*, 0975−7384.
(36) Brüne, B. Nitric oxide: NO apoptosis or turning it ON? *Cell Death Differ.* **2003**, *10* (8), 864−869.
(37) Brüne, B.; von Knethen, A.; Sandau, K. B. Nitric oxide and its role in apoptosis. *Eur. J. Pharmacol.* **1998**, *351* (3), 261−272.
(38) Asahi, M.; Fujii, J.; Suzuki, K.; Seo, H. G.; Kuzuya, T.; Hori, M.; Tada, M.; Fujii, S.; Taniguchi, N. Inactivation of glutathione peroxidase by nitric oxide: implication for cytotoxicity (*). *J. Biol. Chem.* **1995**, *270* (36), 21035−21039.
(39) Maeda, H.; Akaike, T. Nitric oxide and oxygen radicals in infection, inflammation, and cancer. *Biochemistry* **1998**, *63*, 854−865.
(40) Davis, L.; Kuttan, G. Effect of *Withania somnifera* on DMBA induced carcinogenesis. *J. Ethnopharmacol.* **2001**, *75* (2−3), 165−168.
(41) Suraweera, C. D.; Hinds, M. G.; Kvansakul, M. Poxviral Strategies to Overcome Host Cell Apoptosis. *Pathogens* **2020**, *10* (1), 6.
(42) Roos, W. P.; Kaina, B. DNA damage-induced cell death: from specific DNA lesions to the DNA damage response and apoptosis. *Cancer Lett.* **2013**, *332* (2), 237−248.
(43) Rai, N.; Gupta, P.; Verma, A.; Tiwari, R. K.; Madhukar, P.; Kamble, S. C.; Kumar, A.; Kumar, R.; Singh, S. K.; Gautam, V. Ethyl Acetate Extract of *Colletotrichum gloeosporioides* Promotes Cytotoxicity and Apoptosis in Human Breast Cancer Cells. *ACS Omega* **2023**, *8* (4), 3768−3784.
(44) Verma, A.; Rai, N.; Gupta, P.; Singh, S.; Tiwari, H.; Chauhan, S. B.; Kailashiya, V.; Gautam, V. Exploration of *in vitro* cytotoxic and *in ovo* antiangiogenic activity of ethyl acetate extract of *Penicillium oxalicum*. *Environ. Toxicol.* **2023**, *38* (10), 2509−2523.
(45) Kroemer, G.; Galluzzi, L.; Brenner, C. Mitochondrial membrane permeabilization in cell death. *Physiol. Rev.* **2007**, *87* (1), 99−163.
(46) Zilfou, J. T.; Lowe, S. W. Tumor suppressive functions of p53. *Cold Spring Harbor Perspect. Biol.* **2009**, *1* (5), a001883.
(47) Sharma, G.; Kar, S.; Palit, S.; Das, P. K. 18β-glycyrrhetinic acid induces apoptosis through modulation of Akt/FOXO3a/Bim pathway in human breast cancer MCF-7 cells. *J. Cell. Physiol.* **2012**, *227* (5), 1923−1931.

https://doi.org/10.1021/acsptsci.3c00188
ACS Pharmacol. Transl. Sci. XXXX, XXX, XXX−XXX